Cancer Cell International

RESEARCH Open Access

Comprehensive analysis, diagnosis, prognosis, and cordycepin (CD) regulations for GSDME expressions in pan-cancers

Jiewen Fu[1,2†], Dabing Li[1,2†], Lianmei Zhang[1,3†], Mazaher Maghsoudloo[1*], Jingliang Cheng[1*] and Junjiang Fu[1*]

Abstract

The *Gasdermin E* gene (*GSDME*) plays roles in deafness and cancers. However, the roles and mechanisms in cancers are complex, and the same gene exhibits different mechanisms and actions in different types of cancers. Online databases, such as GEPIA2, cBioPortal, and DNMIVD, were used to comprehensively analyze GSDME profiles, DNA methylations, mutations, diagnosis, and prognosis in patients with tumor tissues and matched healthy tissues. Western blotting and RT-PCR were used to monitor the regulation of GSDME by Cordycepin (CD) in cancer cell lines. We revealed that GSDME expression is significantly upregulated in eight cancers (ACC, DLBC, GBM, HNSC, LGG, PAAD, SKCM, and THYM) and significantly downregulated in seven cancers (COAD, KICH, LAML, OV, READ, UCES, and UCS). The overall survival was longer only in ACC, but shorter in four cancers, including COAD, KIRC, LIHC, and STAD, when GSDME was highly expressed in cancers compared with the corresponding normal tissues. Moreover, the high expression of GSDME was negatively correlated with the poor prognosis of ACC, while the low expression of GSDME was negatively correlated with the poor prognosis of COAD, suggesting that GSDME might serve as a good prognostic factor in these two cancer types. Accordingly, results indicated that the DNA methylations of those 7 CpG sites constitute a potentially effective signature to distinguish different tumors from adjacent healthy tissues. Gene mutations for GSDME were frequently observed in a variety of tumors, with UCES having the highest frequency. Moreover, CD treatment inhibited GSDME expression in different cancer cell lines, while overexpression of GSDME promoted cell migration and invasion. Thus, we have systematically and successfully clarified the GSDME expression profiles, diagnostic values, and prognostic values in pan-cancers. Targeting GSDME with CD implies therapeutic significance and a mechanism for antitumor roles in some types of cancers via increasing the sensitivity of chemotherapy. Altogether, our study may provide a strategy and biomarker for clinical diagnosis, prognostics, and treatment of cancers by targeting GSDME.

†Jiewen Fu, Dabing Li and Lianmei Zhang contributed equally to this work.

*Correspondence:
Mazaher Maghsoudloo
Mazaher@swmu.edu.cn
Jingliang Cheng
jinglianngcheng@swmu.edu.cn
Junjiang Fu
fujunjiang@swmu.edu.cn

Full list of author information is available at the end of the article

Keywords The *Gasdermin E* gene, Pan-cancers, Diagnosis, Prognostics, Therapeutics, Cordycepin (CD)

Introduction

The *Gasdermin E* gene (*GSDME*, OMIM: 608798), also named the *deafness autosomal dominant 5* gene (*DFNA5*) and *inversely correlated with estrogen receptor expression 1* gene (*ICERE1*) [1, 2], is located on chromosome 7p15.3. The *DFNA5/GSDME* gene encodes a 496 amino acids GSDME protein with a predicted molecular mass of 54,555 Da [3].

Hearing loss (HL) is among the most hereditary and heterogeneous disorders [4, 5], affecting at least one in every 500 newborns worldwide [6]. Tremendous progress has been achieved for identifying causative genes for hereditary nonsyndromic HL (NSHL) over the past two decades [7, 8]. A gene initially named DFNA5, GSDME, or ICERE1, isolated by Van Laer et al. through a positional cloning strategy, was first identified in 1998 in a Dutch family with NSHL (OMIM: 600994), thereby establishing it is one of the autosomal dominant deafness genes [2, 3]. Recently, we also identified a novel pathogenic variant with a 25 bp insertion in exon 8 of GSDME (p. P372fs*36) in a large Chinese family with autosomal dominant NSHL [9]. GSDME gene comprises 10 exons and spans approximately 60 kb. A 5-prime untranslated region (UTR) of 57 bp precedes the putative translation start site. Van Laer et al. also conducted a Northern blot analysis of 8 human tissues and detected a *GSDME* transcript with a length of 2.2-kb that was highly expressed in the placenta, but showed much lower expression in the heart, brain, and kidney. RT-PCR assays were conducted, detecting mouse *Gsdme* expression in the cochlear epithelial ridge and stria vascularis [3]. Op de Beeck et al. (2011) identified that GSDME has a 3-domain structure: globular domains A, globular domains B, and a hinge region, by comparing gasdermin family members [10]. The GSDME hinge region is situated between globular domain A and globular domain B. Domain A, located at the N-terminus of GSDME, is predicted to have an alpha/beta fold, whereas domain B, located at the C-terminus of GSDME, is predicted to have long alpha-helical structures that may form coiled-coils.

In breast cancer tissues, Thompson and Weigel (1998) found that GSDME expression is inversely correlated with the estrogen receptor [1], suggesting that GSDME may function as a tumor suppressor gene [11–13]. This potential tumor suppressor role for GSDME probably acts by activating pyroptosis and enhancing antitumor immunity [14]. Pyroptosis is a cytogenic necrosis or programmed cell death mediated by pore-forming GSDM proteins, including GSDME, through CASP3 cleaving GSDME or other pore-forming GSDM proteins [15, 16]. However, uncleavable or pore-defective GSDME was not found to be tumor-suppressive. Thus, cancer-associated pyroptosis by GSDME presents a promising avenue for cancer therapeutics by enhancing anti-tumor immunity [14, 17, 18]. Therefore, GSDME could potentially serve as a biomarker in cancers [11, 19].

However, the roles and mechanisms of GSDME in cancers are complex, and the same gene exhibits different mechanisms and roles of action in different types of cancers. An extensive literature review fails to yield a unified conclusion on the results related to GSDME. Pan-cancer analysis of genes, including GSDME, could effectively evaluate the actions of genes such as the *GSDME* gene in different tumors, the predictive value of prognosis, and the survival of cancer patients [20, 21]. Thus, it can better help researchers in different specialties to clarify the overall role of genes in tumorigenesis. Moreover, online databases, including TCGA, GEPIA2, GTEx, and cBioPortal, house a large number of functional genome data settings and mainly focus on the role of these genes in different tumors, which is helpful for our relevant pan-cancer analysis. However, the GSDME expression profiles in pan-cancers are not yet clarified.

Natural products from mushrooms or fungi have a variety of biological activities including anticancer potential. For example, bufalin, a monomer extracted from toadstool, inhibited the occurrence and metastasis of intrahepatic cholangiocarcinoma [22] or gastric cancer [23] through different pathways. Cordycepin (CD), the adenosine analog 3'-deoxyadenosine, was initially isolated from Cordyceps militaris, a popular health food and traditional medicine in China [24, 25]. CD as a natural product, has been demonstrated to possess diverse biological activities, including anti-cancer [26], anti-inflammatory [27], immunomodulatory [28], anti-viral properties. Our previous studies have shown that CD inhibits the cell migration and invasion of triple-negative breast cancer (TNBC) by downregulating transcription factors and inhibits the progression of drug-resistant non-small cell lung cancer (NSCLC) by mediating the AMPK pathways [29, 30]. However, the regulation of GSDME expression by natural products, such as CD, in cancer cells has not been clarified.

In the present study, we aim to comprehensively analyze GSDME expression profiles, DNA methylations, mutations, diagnosis, and prognosis in patients with tumor tissues and matched normal tissues. Additionally, we will investigate the regulation of the GSDME expression by CD has also been studied in various cancer cell lines.

Materials and methods

Online databases

The *GSDME* mRNA and its protein expressions in normal and tumor tissues were retrieved from the Human Protein Atlas (HPA) database (https://www.proteinatlas.org/ENSG00000105928-GSDME) [31, 32]. For further analysis of gene expressions and survival, we utilized GEPIA2 (gene expression profiling interactive analysis), an interactive web server derived from the Genotype Tissue Expression (GTEx) program and TCGA. Gene expression profiles were obtained through GEPIA2 (http://gepia2.cancer-pku.cn/#index) [33–35], allowing us to compare GSDME expression in tumors and matched normal tissues.

The cBioPortal is a comprehensive platform that facilitates the visualization and analysis of cancer Genomics, including mutations and survival data for GSDME. Mutational hotspots analysis of GSDME and survival analysis were conducted using cBioPortal [36]. To provide more detail, we accessed the website (https://www.cbioportal.org/), inputted the gene name "GSDME", selected the icons for "mutations", "comparison/survival", and "survival", and obtained survival plots along with corresponding *p*-values. For GSDME DNA methylation, as well as diagnostic and prognostic model analysis, we utilized the DNA Methylation Interactive Visualization Database (DNMIVD) (http://119.3.41.228/dnmivd/diagnosis/) [37].

The validation of GSDME expression with external datasets

We used more than 15 datasets from GEO and ArrayExpress gene expression databases to validate GSDME expression. We selected a dataset that included both healthy and tumor samples. We conducted a differential gene expression (DEG) analysis to detect upregulated and downregulated genes. Most of these analyses were performed using GEO2R, but some were analyzed using the Limma R package.

Protein-protein interaction network

We used the STRING online database (https://string-db.org/) to extract physical protein-protein interactions (PPI) between the GSDME protein and other proteins and to reconstruct the co-expression network [38]. Initially, we entered this gene as input into the database. We only considered experimental interactions and disabled the other options. Additionally, we set the medium confidence score to 0.7 and considered a maximum of interactors at three levels: (1) default, (2) 1st shell, and (3) 2nd shell.

Enrichment analysis

To understand the biological, functionality and mechanism of GSDME expression, we utilized the ToppGene online database (https://toppgene.cchmc.org/) to enrich this gene based on biological criteria, including: gene ontology (GO), pathways, molecular functions (MF), diseases, drugs, and etc.

Cell growth, invasion, and migration assays

MCF7 and H460 cells, purchased from ATCC, USA, were then evenly seeded in 12-well plates and cultured in a 37 °C, 5% CO_2 incubator. The cells were grown in DMEM medium with 10% FBS and 1% penicillin / streptomycin. Transfection of plasmids, pCMV-EGFP-GSDME (human)-Neo vector (cat: P39523, Miaoling Biology, China) and its empty vector was performed when the cell density reached 60–70%. After 24 h, the cells were directly used for the CCK-8 proliferation assay using CCK-8 kit (cat: K1018, APExBIO, USA).

The Matrigel matrix gel (cat: 356234, Corning, USA) was diluted with pre-cooled serum-free medium to achieve a concentration of 1.0 mg/ml. In the transwell plates, added 60 µl of the diluted Matrigel matrix gel was added to the invasion chamber for 2 h in a 37 °C, 5%CO_2 incubator. MCF7 and H460 cells were seeded in the upper chamber, and 600 µl of medium containing 20% FBS was added to the lower chamber to establish a chemotactic gradient, with a volume of 200 µl per well. After 48 h of incubation, in the incubator, the invasion chamber was removed, the supernatant was discarded, and cells on the surface of the small chamber were removed with a cotton swab. The chamber was then placed in a fixative solution for 10 min at room temperature, followed by two rinses using 1×PBS. Subsequently, the invasion chambers were placed in a 0.5% crystal violet staining solution (cat: C0121, Beyotime Biotechnology, China), stained at room temperature for 5 min, and rinsed twice using PBS. The compartments were observed using a microscope, photographed, and cells were counted.

In contrast to the transwell cell invasion assay, the migration assay was performed similarly to the cell invasion assay, with the exception that Matrigel matrix gel was not used.

Cell culture and cordycepin (CD) treatments

The lung cancer cell line A549 was also purchased from ATCC, USA. Both A549 and MCF7 cell lines were cultured with DMEM medium (Gibico, USA), containing 10% FBS and 1% penicillin/streptomycin. CD was purchased from Must Bio-Technology Co. Ltd (Chengdu, Sichuan, China and had been used in previous studies [29, 39, 40]. The cell lines were cultured in a 12-well plate and treated with CD at final concentrations (µM) of 0, 10, 20, and 40 for 24 h. Proteins were lysed, and their expression was examined by western blotting. Total RNA was extracted for reverse transcription and RT-PCR [20, 39].

Western blot assays

After lysing with EBC buffer and boiling at 100 °C for 5 min, the protein samples underwent electrophoresis in the Bio-Rad Mini PROTEAN Tetra System (Bio-Rad, USA). Subsequently, the samples were transferred to PVDF membranes and washed twice with 1×TBST buffer. The membranes were then blocked with 5% free-fat milk for 1 ~ 2 h at room temperature. The primary antibodies for DNFA5/GSDME (cat no: 67731-1-Ig) and GAPDH (cat no: 60004-1-Ig) from Proteintech Group, Inc (Wuhan, China) were diluted with 2% free-fat milk at ratios of 1:5000 and 1: 10,000 respectively. Then, the membranes were incubated with the diluted primary antibodies overnight at 4 °C. The membranes were washed for 15 min thrice and the secondary antibodies were then incubated for 2 h. After an additional three washes, the bands were imaged as described previously [30, 41].

RT-PCR amplification

The total RNA from cultured cell lines was extracted using the kit from Tiangen Biochemical Technology (Beijing) Co., LTD (cat.no.: #DP419, Beijing, China), then cDNA was reverse transcribed using an RT kit (TOYOBO, China) and ReverTra Ace®qPCR RT Master Mix (cat.no.: FSQ-201, Shanghai, China) from Oriental Textile (Shanghai) Biotechnology Co., LTD. The forward primer RT-DFNA5-L: gccacaacagacagctttga and the reverse primer RT-DFNA5-R: cagacagagcacgaagcaag for GSDME were designed using the Primer3 online website and applied for PCR amplification with 30 cycles. The RT-PCR product size for GSDME is 362 bp, with ACTB serving as an internal control and performed it for PCR amplification with 23 cycles. PCR amplification was performed using a Veriti 96 well thermal cycler (ABI, USA), followed by electrophoresis on a 1.5% agarose gel with 10,000:1 dilution GoldView II from Beijing Solarbio Science & Technology Co.,Ltd. (cat.no.: G8142, Beijing, China) [20].

Statistical analysis

In the survival analysis, GSDME expressions of individuals were divided into high-and low-expression groups using the median expressions. A Logrank test with $p<0.05$ was considered as a significant difference.

Results

GSDME expression in tumor tissues and the corresponding tissues in pan-cancers

In 33 types of cancers, GSDME expressions were significantly upregulated in eight cancers, including ACC (Adrenocortical carcinoma), DLBC (Lymphoid Neoplasm Diffuse Large B-cell Lymphoma), GBM (Glioblastoma multiforme), LGG (Brain Lower Grade Glioma), HNSC (Head and Neck squamous cell carcinoma), PAAD (Pancreatic adenocarcinoma), SKCM (Skin Cutaneous Melanoma), and THYM (Thymoma) (Fig. 1A, B, $p<0.05$). They were significantly downregulated in seven cancers, including COAD (Colon adenocarcinoma), KICH (Kidney Chromophobe), LAML (Acute Myeloid Leukemia), OV (Ovarian serous cystadenocarcinoma), READ (Prostate adenocarcinoma), UCES (Uterine Corpus Endometrial Carcinoma), and UCS (Uterine Carcinosarcoma) compared with the corresponding healthy tissues (Fig. 1A, C, $p<0.05$). Then, we performed IHC for GSDME in lung adenocarcinoma tissues, and results showed that it is ubiquitously expressed in the cytoplasm of lung tumor cells (Fig. 1D and E), while negative control without GSDME antibody showed no signal (Fig. 1F).

Then, we conducted validation through a differential gene expression (DEG) analysis, and the results are shown in Table 1. Cancers marked in red indicate upregulation of the *GSDME* gene, while cancers marked in green indicate down-regulated expression. It is worth noting that cancers marked in black do not show significant differences between cancer and healthy samples. Some datasets did not reach statistical significance; however, we used multiple datasets to ensure the reliability of the results. Thus, we confirmed that GSDME expressions were significantly upregulated in ACC, DLBC, GBM, LGG, HNSC, PAAD, SKCM, and THYM; and were significantly downregulated in COAD, KICH, LAML, OV, READ, and UCES compared with the corresponding healthy tissues.

Prognostic values for GSDME expression in pan-cancers

According to the expressions of GSDME, the tumor patients were divided into high- and low-expression groups for survival analysis. The correlation between GSDME expression and prognosis in different types of tumors was further performed, and the results are shown in Fig. 2. The overall survival is longer only in ACC (Fig. 2A, Logrank $p=0.021$), while it is shorter in four cancers, including COAD (Fig. 2B, Logrank $p=0.029$), KIRC (Kidney renal clear cell carcinoma) (Fig. 2C, Logrank $p=0.032$), LIHC (Liver hepatocellular carcinoma) (Fig. 2D, Logrank $p=0.0018$), and STAD (Stomach adenocarcinoma) (Fig. 2E, Logrank $p=0.0077$), when GSDME is highly expressed in cancers compared with the corresponding normal tissues. As a consequence, the high expression of GSDME was negatively correlated with the poor prognosis of ACC, while the low expression of GSDME was negatively correlated with the poor prognosis of COAD, suggesting that GSDME might be a good prognostic factor in these two cancer types.

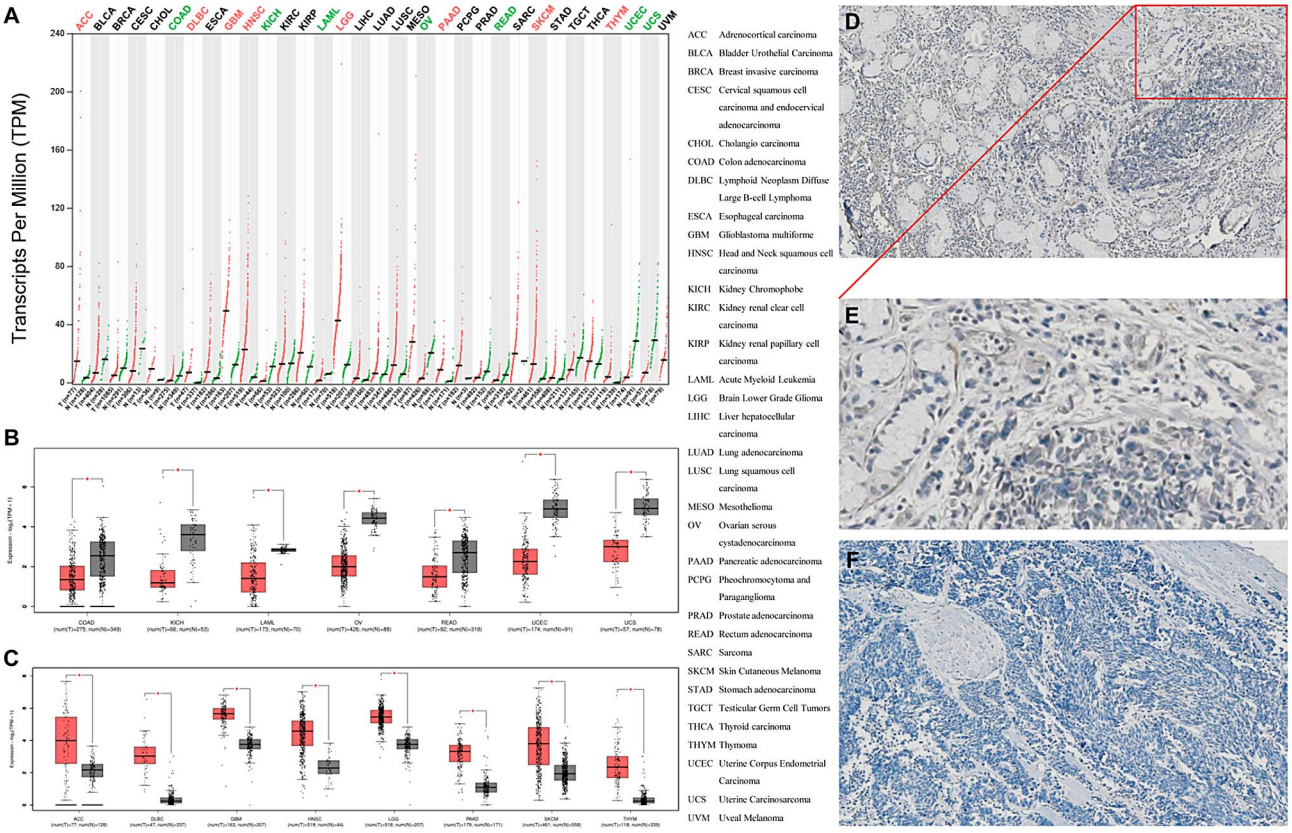

Fig. 1 Expressions and localization of GSDME in pan-cancers and the corresponding normal tissues. **A**. The profiles of GSDME in 33 cancer types by dot plots. "T" indicates tumors, while "N" indicates the corresponding normal tissues. The right panel shows the full names in pan-cancers. **B**. The profiles of GSDME with significant increases in eight cancer types by heatmaps. **C**. The profiles of GSDME with significant decreases in seven cancer types by heatmaps. D ~ F. Immunohistochemistry (IHC) in lung adenocarcinoma tissues using GSDME antibody **D**, enlarged image from panel D **E**, and control without GSDME antibody staining **F**. IHC was performed in lung adenocarcinoma tissues using GSDME antibody (cat no: 67731-1-Ig, Proteintech Group, Inc, Wuhan, China)

Table 1 The validation of GSDME expression in multiple external datasets

Cancer	GEO	ArrayExpress	Adj.*P*.value	*P*.Value	LogFold	UP/DOWN
Adrenocortical Cancer (ACC)	GSE75415	E-GEOD-75,415	2.08E-01	4.00E-02	0.9418	UP
Large B-cell Lymphoma (DLBC)	GSE145842	---	1.39E-02	2.63E-04	1.3531	UP
Glioblastoma (GBM)	GSE50161	E-GEOD-50,161	6.37E-02	4.63E-02	0.3256	UP
Head and Neck Cancer (HNSC)	GSE30784	E-GEOD-30,784	1.00E-20	2.16E-22	2.6400	UP
Lower Grade Glioma (LGG)	GSE26576	E-GEOD-26,576	0.2267	2.34E-02	0.8579	UP
Pancreatic Cancer (PAAD)	GSE62165	---	3.22E-17	2.19E-18	2.1200	UP
Melanoma (SKCM)	GSE114445	---	0.0346	5.16E-03	0.8929	UP
Thymoma (THYM)	GSE79978	---	2.54E-02	1.12E-03	0.8854	UP
Colon Cancer (COAD)	GSE75970	---	0.0403	0.0113	-2.50	DOWN
Kidney Chromophobe (KICH)	GSE15641	E-GEOD-15,641	5.22E-04	8.04E-05	-0.6391	DOWN
Acute Myeloid Leukemia (LAML)	GSE35010	E-GEOD-35,010	3.46E-02	1.86E-03	-0.3470	DOWN
Ovarian Cancer (OV)	GSE26712	E-GEOD-57,342	3.11E-43	2.93E-46	-3.3407	DOWN
Rectal Cancer (READ)	GSE75970	---	0.0593	0.0249	-0.2572	DOWN
Endometrioid Cancer (UCEC)	GSE25427	E-GEOD-25,427	0.140833	1.92E-02	-0.7475	DOWN
Uterine Carcinosarcoma (UCS)	---	E-MTAB-7039	0.0004	---	-1.4000	DOWN

Results for diagnostic model construction on the *GSDME* methylation in pan-cancers

Methylations of the *GSDME* gene are frequently detected in colorectal carcinoma [12, 42], and they have been associated with an increased metastatic risk in breast cancer carcinoma [43]. Therefore, we aim to investigate whether the *GSDME* methylation can serve as a diagnostic model in pan-cancers. Figure 3 presents a

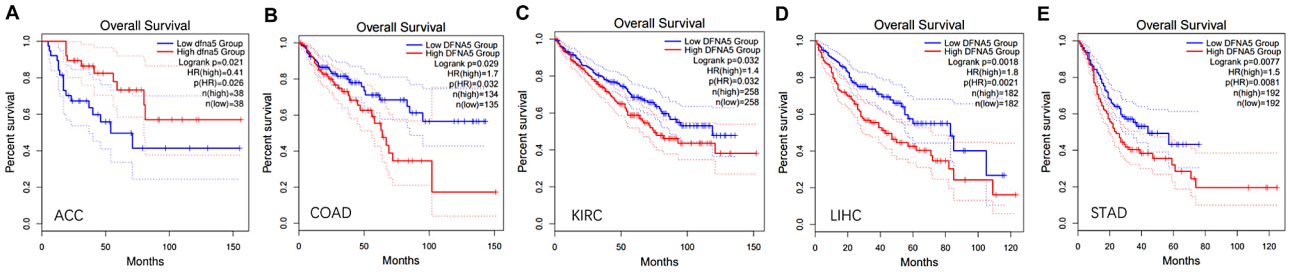

Fig. 2 The prognostic values of GSDME expression for ACC **A**, COAD **B**, KIRC **C**, LIHC **D**, and STAD **E**. The middle panel of Fig. 1 provides the full names in pan-cancers

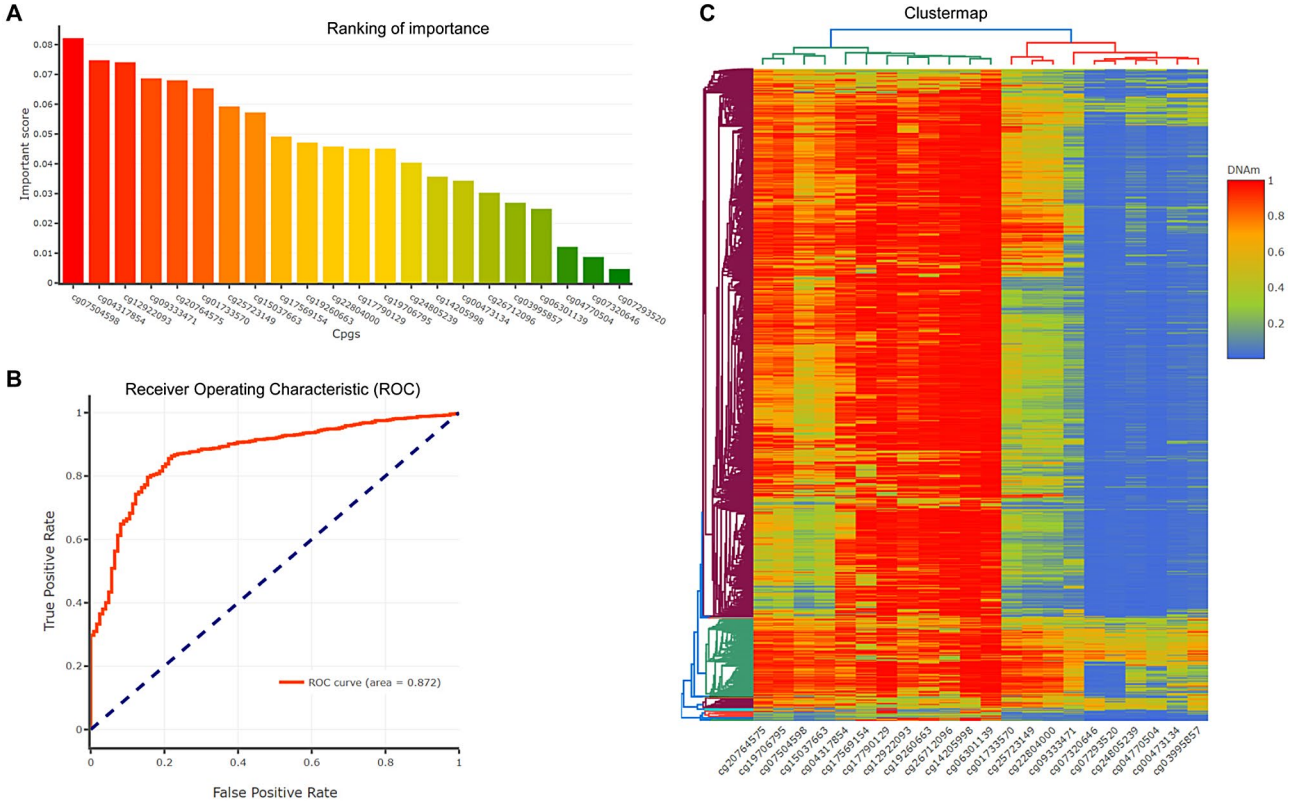

Fig. 3 Construction of the diagnostic model on the GSDME methylations. **A** Barplots of a diagnostic model for pan-cancers on the GSDME methylations, showing a ranking of importance for every CpGs in GSDME. **B** ROC curve of the high sensitivity and specificity in distinguishing different types of cancers from the matched normal tissues. **C** Unsupervised hierarchical clustering and heatmap of the profiles of GSDME methylations for these 22 CpGs among all samples of 23 cancers and the matched normal samples. Left color bars mark the tissues of cancer types

ranking of importance (important score > 0) for 22 CpGs in GSDME, along with a Receiver Operating Characteristic (ROC) curve and a clustering map for distinguishing tumor samples from normal samples in 23 types of cancers. The importance for GSDME CpGs indicates that CpG cg07504598 has the highest importance score > 0.08, while cg07293520 has the lowest < 0.01 (Fig. 3A). In the logistic regression model, the diagnostic value evaluated by the ROC curve yielded an Area Under Curve (AUC) of 0.872 (Fig. 3B), implying that this model can effectively discriminate tumor individuals from normal samples. Clustering heatmaps illustrating the profiles of *GSDME* methylations for these 22 CpGs among tumor and healthy samples are shown in Fig. 3C. Notably, the significantly differentially methylated probes could successfully discriminate each cancer type from the others as well. Consequently, these results suggest that the DNA methylations of these 7 CpG sites constitute a potentially effective signature to discriminate different tumors from adjacent healthy tissues.

Results for prognostic model construction on the GSDME methylation in pan-cancers

To construct an effective prognostic model for different cancer types, we performed a series of feature selections with stringent criteria, as described previously [44]. After filtering, only several potential signatures were identified. We observed that probes were identified in 5 different cancers, including CESC (cg17569154), KIRC (cg01733570, cg04317854, and cg07504598), SKCM (cg09333471), STAD (cg20764575 and cg26712096), and THYM (cg04317854 and cg12922093) (p value$<$0.01). Subsequently, we divided all the patients into high-risk or low-risk groups using the median partial hazard as the cutoff (Fig. 4). In comparison to the low-risk group, patients in the high-risk group showed significantly shorter OS in 5 cancers (Fig. 4B, upper panel, p-value$<$0.01). Further analysis revealed that patients with lower Z-scores generally had better outcomes than those with higher risk scores (Fig. 4, lower panel). Consequently, we have successfully developed a probe-based prognostic model capable of effectively categorizing tumor individuals into high and low risk, corresponding to shorter and longer OS, respectively, grounded on the partial hazard in 5 different cancer types (Fig. 4).

Genetic alterations for GSDME and the prognostics

GSDME mutations have been implicated in causing aging-related hearing loss. Subsequently, we conducted an analysis of genetic alterations for GSDME in the pan-cancers using the cBioPortal (TCGA, Pan-Cancer Atlas). In this analysis, the "Cancer Types Summary" module was used to observe the genetic alteration frequency in 32 cancers, encompassing mutation, amplification, structural variant, deep deletion, multiple alterations, and CNA in all TCGA tumors. The results found that GSDME mutations are most prevalent in UCES at 6.99% (529 cases), with mutations accounting for 5.48% in 29 cases, amplification at 1.32% in 7 cases, and deep deletion at 0.19% in 1 case. Conversely, GSDME mutations are least frequent in Kidney Renal Clear Cell Carcinoma (KIRC) at 0.1% (mutation observed in 0.1% in 1 case) (Fig. 5A). No GSDME genetic alterations were shown in the other 7 cancer types, including Thymoma, Mesothelioma, KICH, Uterine Carcinosarcoma, LAML, DLBC, and CHOL (cholangiocarcinoma) (Fig. 5A). The most common type of gene alteration was "Amplification", followed by "Mutation" and "Deep Deletion". Subsequently, we used the "Mutation" module to examine the mutation frequency and types, which included missense, truncating, inframe, splice, fusion, and a total of 115 mutations with somatic mutation frequency of 0.9%. These mutations comprised 94 missenses, 12 truncations, 1 inframe, 6 splices, and 2 fusions, distributed across the entire *GSDME* gene, predominantly in the Gasderm in domain (Fig. 5B). Among these Post Translational Modifications (PTMs) site mutations, 4 were located at phosphorylation sites, 1 located at the ubiquitination site, and 1 located at the S-nitrosylation site (Fig. 5B).

We also investigated the potential correlation between DNA alterations in GSDME and the prognosis of various types of cancers. Kaplan-Meier analysis revealed that patients with DNA alterations in GSDME have unfavorable OS, disease-specific survival (DSS), and progression-free survival (PFS) compared to patients without mutations. However, no significant differences were found in all three survival measures between the DNA -altered and unaltered groups, although the median months were shorter (Figs. 5C and 95% CI, $p>0.05$). These data imply that GSDME is mutated in most cancers but doesn't exhibit prognostic significance.

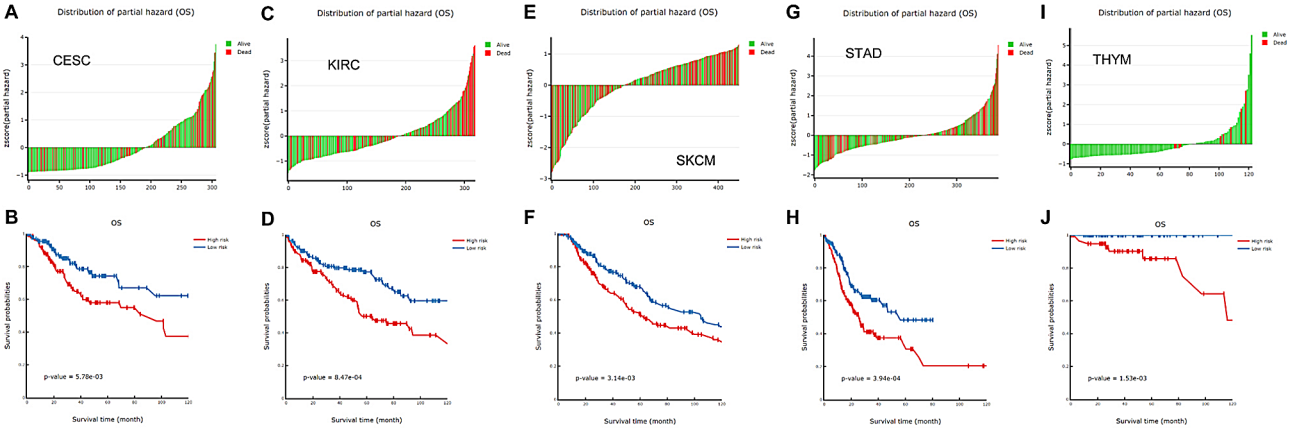

Fig. 4 Construction of the prognostic model on the GSDME methylation. **A**~**J**. The prognostic classifier results in 5 cancer types, respectively. **A**, **C**, **E**, **G**, **I**: Z-scores distribution of the prognostic classifier and the status for patient survival with indicated types of cancers, respectively. **B**, **D**, **F**, **H**, **J**. Kaplan-Meier survival analysis in 5 cancers. We divided the patients into low-risk and high-risk groups using the median cutoff value of the partial hazard. p-value was calculated by the log-rank test

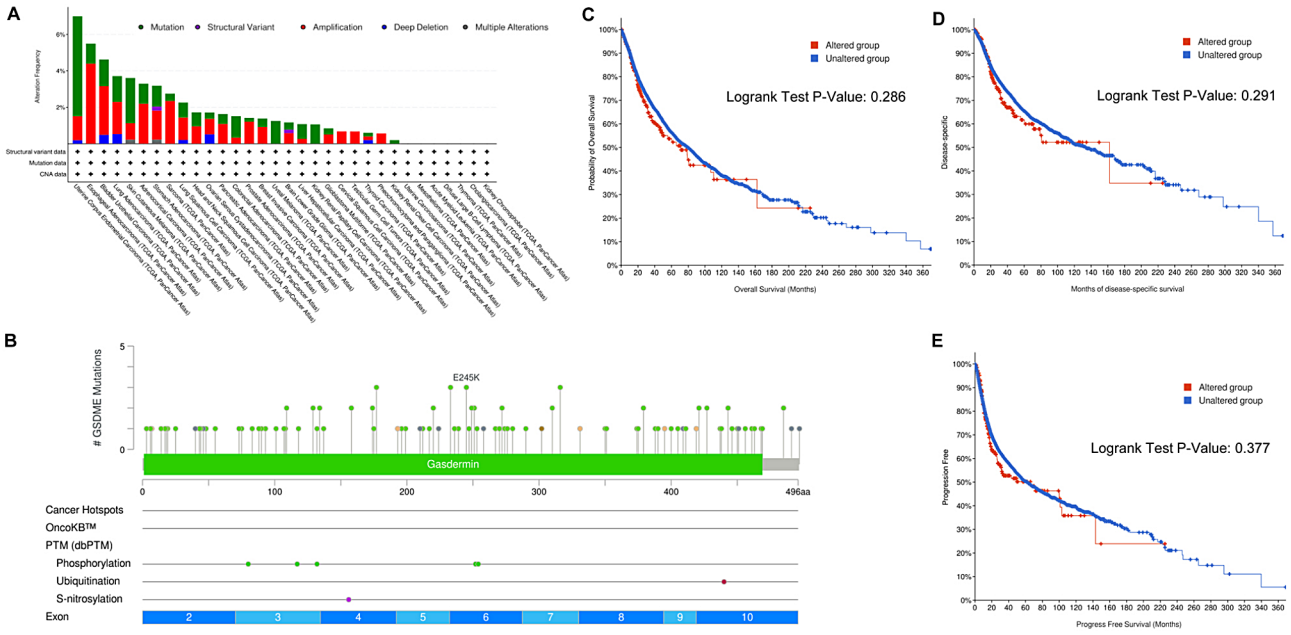

Fig. 5 Genetic alteration feature of GSDME in pan-cancers of TCGA. **A**. Alteration frequency in GSDME with the different genetic alteration. The results are shown through the cBioPortal tool. **B**. GSDME genetic alteration and its locations for pan-cancers. **C** ~ **E**. Association of GSDME mutation status and overall, disease-specific, disease-free, and progression-free survivals of cancer patients, respectively. The detailed P values are shown in Fig. 5C ~ E respectively

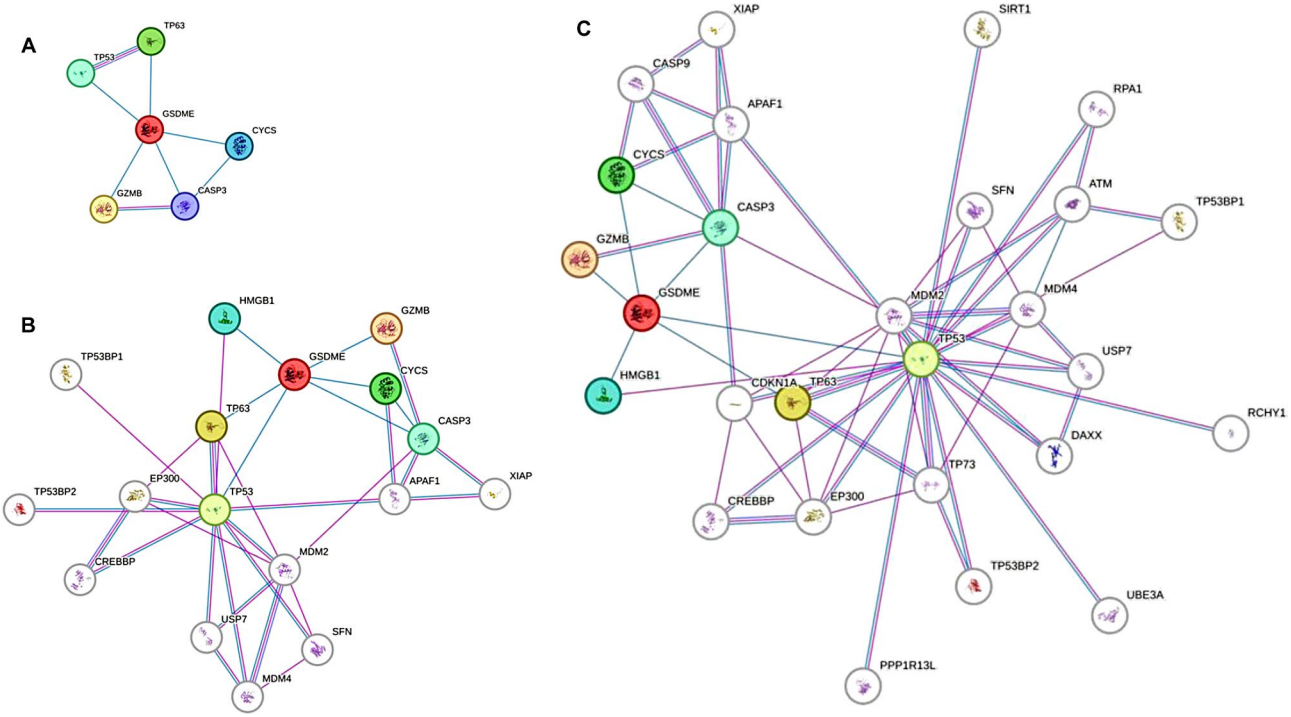

Fig. 6 PPI co-expression network: Networks were extracted from the STRING database at three levels. **A**. The PPI network with maximum interactors was extracted using default parameters. **B**. The PPI network was extracted with the maximum interactors set to the first shell. **C**. The PPI network with maximum interactors was extracted on the second shell

Protein-protein interaction network

To reconstruct the co-expression network, we used the STRING online database to extract PPI between the GSDME protein and other proteins. The results are shown in Fig. 6, and we found that GSDME directly interacts with the TP53, TP63, CYCS, GZMB, and CASP3 proteins, indicating a direct correlation with these genes when using STRING. It is likely that CD

mediates GSDME expression and activation through a number of different mechanisms. Through TP53 activation, CD can enhance GSDME transcription [45]. Moreover, CD can trigger the intrinsic apoptotic pathway by releasing CYCS, which triggers the cleavage of GSDME and activates caspase-3 [46]. Furthermore, by increasing GZMB activity through its effects on immune cells, CD can directly cleave GSDME [47]. These interactions demonstrate how CD can modulate cell death pathways via an intricate regulatory network. Because of this characteristic, CD may prove to be a useful drug in the treatment of illnesses like cancer that are associated with dysregulated cell death. However, we explored numerous links between GSDME protein and other proteins, both directly and indirectly, in the first and second shell, revealing their involvement in cancers.

The results of the enrichment analysis

To understand the functional roles and biological mechanism of GSDME protein, we utilized the ToppGene online database to enrich this gene based on biological criteria, including GO pathways, MF, diseases, drugs, and etc. We found that multiple pathways involved in cancers were enriched for GSDME, including the release of apoptotic factors from the mitochondria, pyroptosis, toll-like receptor cascades, programmed cell death, and regulated necrosis. Also, this gene was enriched for various biological processes such as positive regulation of response to tumor cells, regulation of immune response to tumor cells, positive regulation of the intrinsic apoptotic signaling pathway, mechanoreceptor differentiation, and epidermal cell differentiation. The results of this analysis are reported in Table S1.

CD treatment suppresses GSDME expression in A549 and MCF7 cancer cells

To assess whether CD affects GSDME expression for its therapeutic potential, we treated the lung cancer cell line (A549) and breast cancer cell line (MCF7) with different concentrations CD (0, 10, 20, and 40 μM) for 24 h and performed western blotting. The results, as depicted in Fig. 7, indicate that CD dose-dependently suppresses the protein expressions of GSDME, while the mRNA levels remain unaffected in both A549 (Fig. 7A, B, C) and MCF7 (Fig. 7D, E, F), respectively. Subsequently, we investigated whether CD inhibits GSDME expression in vivo. Mice were divided into the experimental group with CD treatment and control group without CD treatment. Spleen lymphocytes were isolated for western blotting and semi-quantitative PCR, and the results are shown in Supplementary Fig. 1, suggesting that CD may inhibit Gsdme protein expression, but not mRNA expression, in mice (Supplementary Fig. 1). Of course, the expression of GSDME analyzed in other organs of mice after CD treatment, not only in the spleens, can be tested in the future.

GSDME may promote cell migration and invasion in both MCF7 and H460 cancer cells

To investigate whether GSDME could affect cancer cell proliferation, migration, and invasion, we first

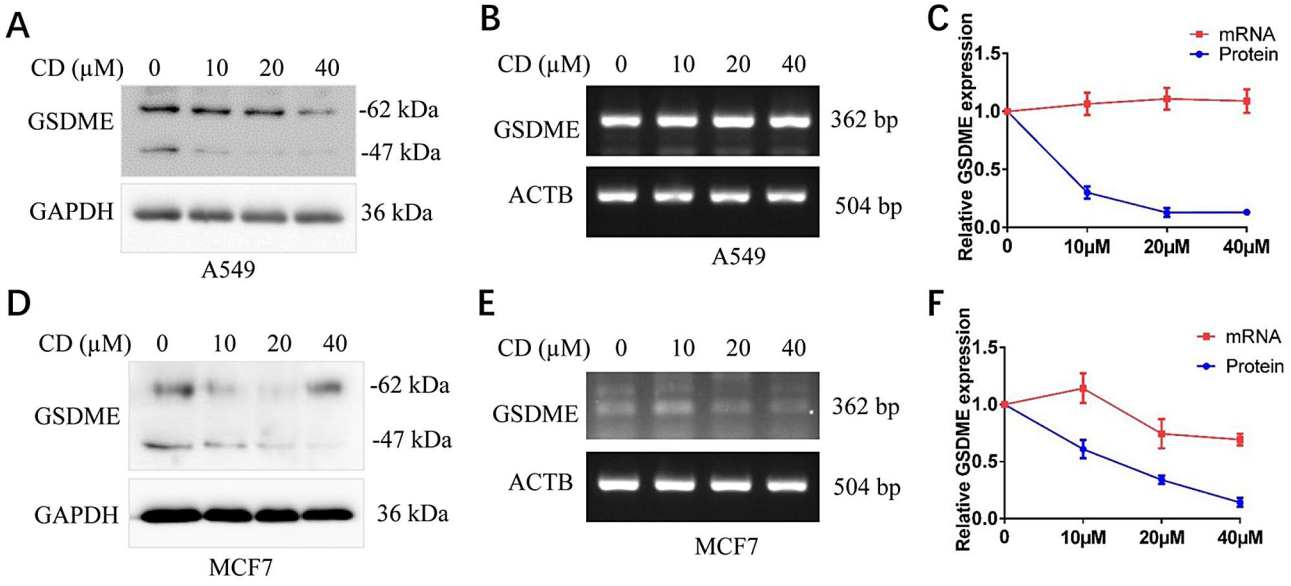

Fig. 7 GSDME expressions by CD in cancer cell lines. **A**. GSDME protein expressions by CD treatment in cancer cell line A549. **B**. GSDME mRNA expressions by CD treatment in cancer cell line A549. **C**. Quantitative results for panel A and B. **D**. GSDME protein expressions by CD in cancer cell line MCF7. **E**. GSDME mRNA expressions by CD in cancer cell line MCF7. F. Quantitative results for panels D and E. Red lines indicate GSDME mRNA expressions while blue lines indicate GSDME protein expressions. High molecular weight bands with indicated approximately 62 kDa are possibly uncleaved ones and low molecular weight bands with indicated approximately 47 kDa could be the cleaved ones, which present in panels A and D

overexpressed GSDME in the breast cancer cell line MCF7. However, the overexpression of GSDME did not significantly promote cell proliferation in MCF7 (Data not shown). Consequently, we used both the lung cancer cell line H460 and MCF7 for migration and invasion assays. The results are shown in Fig. 8, indicate that overexpression of GSDME significantly promoted cell migration and invasion in both MCF7 (Fig. 8A, B) and H460 (Fig. 8C, D), respectively. Western blot analysis confirmed the successful overexpression of GSDME (Supplementary Fig. 2 and data not shown).

Discussion

The actions and mechanisms within cancers are complex, and the same gene may have different mechanisms and actions in different types of cancers, including GSDME. Pan-cancer analysis of GSDME could effectively evaluate the roles in different tumors, the predictive value of prognosis, and the survival of cancer patients [20, 21]. In this study, we found that GSDME expression is significantly increased in eight cancers (ACC, DLBC, GBM, HNSC, LGG, PAAD, SKCM, and THYM); and is significantly downregulated in seven cancers (COAD, KICH, LAML, OV, READ, UCES, and UCS), compared with the corresponding normal tissues. The overall survival is longer only in ACC, but shorter in four cancers including COAD, KIRC, LIHC, and STAD when GSDME was highly expressed in cancers compared with the corresponding normal tissues. Moreover, the high expression of GSDME was negatively associated with the poor prognosis of ACC, while the low expression of GSDME was negatively associated with the poor prognosis of COAD, which might be a good prognostic factor in these two cancer types. Accordingly, these results indicate that the levels DNA methylations at those 7 CpG sites constitute a potentially effective signature to discriminate different tumors from adjacent healthy tissues. We found that probes identified in 5 different cancers including, CESC (cg17569154), KIRC (cg01733570, cg04317854, and cg07504598), SKCM (cg09333471), STAD (cg20764575 and cg26712096), and THYM (cg04317854 and cg12922093). Additionally, we observed that the patients with lower Z-scores generally have better outcomes than those with higher risk scores. Altogether, we systematically and successfully clarified the GSDME expression profiles, diagnostic values, and prognostic values in pan-cancers. This information can significantly assist researchers in different specialties to better understand the overall role of genes in tumorigenesis.

Both TP53 and TP63 belong to the same family and function as crucial tumor suppressors in cancer prevention. They regulate the cell cycle, serving as checkpoints to inhibit uncontrolled cell division. In response to DNA damage or mutations, these genes can either pause the cell cycle for DNA repair or trigger apoptosis, eliminating damaged cells. Therefore, the direct link between TP53/TP63 and GSDME suggests that this protein may have a vital effect in cancers [48]. CYCS, a gene encoding a protein essential for the cell's energy production through the electron transport chain, is situated in mitochondria, where it regulates cell apoptosis (programmed cell death). Disruptions in this process can enable cancer cells to evade apoptosis, promoting their uncontrolled growth and survival. Thus, the association between CYCS and

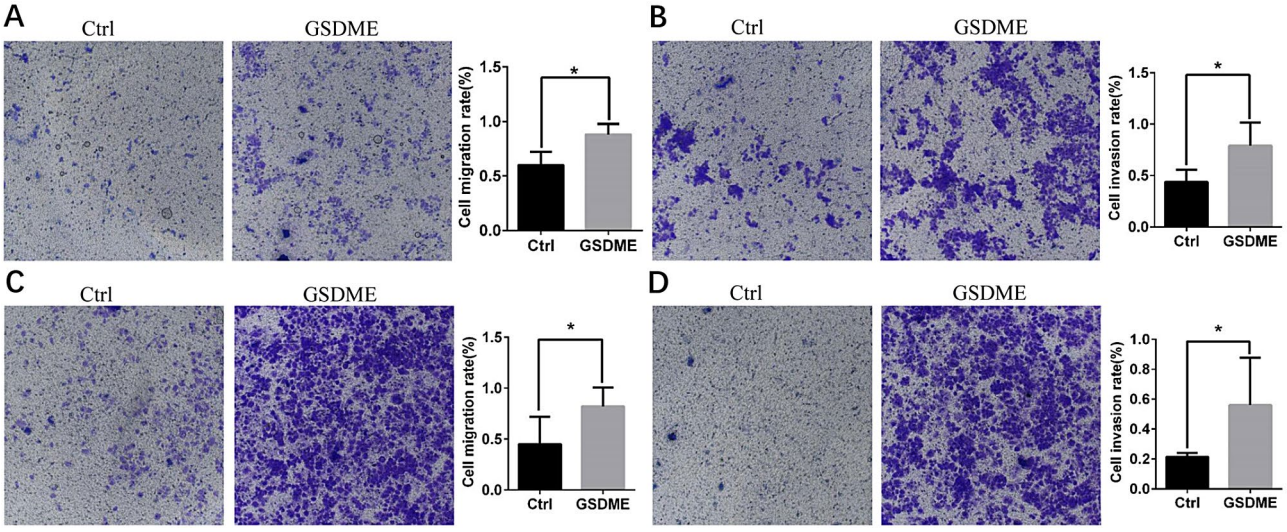

Fig. 8 GSDME promotes cell migration and invasion in both breast cancer cells MCF7 and lung cancer cells H460. **A**. GSDME promotes cell migration in MCF7. **B**. GSDME promotes cell invasion in MCF7. Quantitative results are shown in right panels. **C**. GSDME promotes cell migration in H460. **D**. GSDME promotes cell invasion in H460. Quantitative results are shown in right panels. "*" indicates the $p < 0.05$. Ctrl, empty vector without overexpression of GSDME; GSDME, overexpression of GSDME

GSDME could have a significant impact on cancer development [49]. CASP3, a key enzyme in apoptosis, is activated during this process and aids in cell dismantling by cleaving specific proteins, leading to cell death and removal. Disruptions in apoptosis regulation are common in cancers, where mutations in genes like CASP3 enable cancer cells to evade cell death and sustain uncontrolled growth [50]. Therefore, the relationship between this gene and GSDME could have a crucial impact on cancer development.

In healthy cells, mitochondria release pro-apoptotic proteins such as cytochrome c in response to various signals, including DNA damage or cellular stress. Once released into the cytoplasm, cytochrome c initiates a series of events that lead to the activation of caspases and, ultimately, cell death. The release of apoptotic factors from the mitochondria is one of the pathways enriched for GSDME. In cancer cells, disruptions in mitochondrial function, mutations in pro-apoptotic proteins, and alterations in the expression of anti-apoptotic proteins like Bcl-2 and Bcl-xL can interfere with the apoptotic process. Consequently, cancer cells can evade apoptosis, leading to uncontrolled proliferation and survival [51]. Pyroptosis, a programmed cell death process, is integral to the body's immune response against infections. In contrast to apoptosis, which is controlled and non-inflammatory, pyroptosis involves rapid cell lysis and the release of pro-inflammatory cellular contents. Inflammasomes, multiprotein complexes sensing pathogen-associated molecular patterns (PAMPs) or danger-associated molecular patterns (DAMPs), trigger pyroptosis. Activated inflammasomes induce caspase-1 activation, leading to gasdermin D cleavage, cell membrane rupture, and the release of pro-inflammatory cytokines like interleukin-1 beta (IL-1β) and interleukin-18 (IL-18). Recent studies have shown that pyroptosis is involved in the inflammation and tumor progression of cancers [52].

Mechanoreceptor differentiation is one of the biological processes enriched for the GSDME protein. Mechanoreceptor differentiation is crucial in diverse physiological processes such as tissue development, homeostasis, and immune responses. However, disruptions in mechanoreceptor differentiation pathways have been linked to cancer progression and metastasis. These alterations can impact cell behavior, including migration, invasion, and resistance to apoptosis. Dysregulated mechanoreceptor signaling is associated with heightened cancer cell motility, enabling their spread to distant tissues. Moreover, changes in mechanoreceptor differentiation might influence the tumor microenvironment, fostering tumor growth and angiogenesis [53, 54].

The abnormal expression of GSDME frequently occurs in multiple types of tumors, and regulating GSDME expression may be one of the methods to improve the therapeutics and the prognosis of patients. When GSDME is highly expressed, cytotoxic drugs can induce tumor cell death through caspase-3-dependent pyroptosis [55]. Liu et al found that GSDME is highly expressed in head and neck squamous cell carcinoma (HNSCC) tissues and correlated with worse survival [56]. Recent studies have also found GSDME that is highly expressed in PDAC tissues and positively correlated with vascular invasion, PDAC progression, and chemoresistance by promoting invasion and metastasis [57]. Thus, a high level of GSDME may increase the side effects of chemotherapeutic drugs [55]. The CD is the adenosine analog 3'-deoxyadenosine, isolated from *Cordyceps militaris*, which is a popular health food and traditional medicine in China [24, 25]. CD is a natural product showing broad biological activities, such as anti-inflammatory [27], anticancer [26, 58], and immunomodulatory [28]. Moreover, numerous studies have indicated that CD has anticancer and antimetastatic capability in various cancers in vitro and in vivo [59–61], with therapeutic potential [62, 63]. Others or our previous studies indicated that CD inhibited cancer progress and cancer metastasis through different target genes or pathways, such as epithelial-to-mesenchymal transition (EMT)-inducing transcription factors (TWIST1, SLUG, SNAIL1, and ZEB1) [30], AMPK Signaling Pathway [29], SARS-CoV-2 receptors (TMPRSS2, ADAM17, CTSL, NRP1, CD26, and CD147) [20, 39, 64, 65], AKT, ERK, PI3K, and GSK-3β/β-catenine [66], et.c. We thus want to know whether CD affects GSDME expression. Interestingly, when CD was treated GSDME expression was inhibited in different cancer cell lines, demonstrating the possible therapeutic mechanism by targeting GSDME in some types of cancers via increasing the sensitivity to chemotherapy.

Moreover, genetic mutations could play critical roles in the mechanism of carcinogenesis. Genetic mutations in the GSDME gene are frequently observed in various tumors, with the highest occurrence in UCES. Gene alteration types include amplification, mutation, structural variant, deep deletion, multiple alterations, and CNA in all TCGA cancers. "Amplification" was the most common type of gene alteration, followed by "mutation" and "deep deletion". Genetic mutation may effectively predict the occurrence of adverse prognostic events in cancer patients. However, the mechanism of action between GSDME mutations and the prognosis of cancer patients should be further explored using more samples in the future, along with assessing the feasibility of GSDME as a therapeutic target.

However, more evidence, approaches, or experiments should be conducted to demonstrate whether targeting GSDME with CD, a traditional Chinese medicine, holds therapeutic significance for antitumor roles in some

types of cancers by increasing sensitivity to chemotherapy or through effective drug delivery systems [67].

Conclusions

Collectively, a series of pan-cancer analyses were performed to determine the relevance of GSDME in pan-cancer and its potential predictive value. We revealed that the expression of GSDME is related to clinical values for the diagnostics and prognosis of tumor cells. The gene mutations for GSDME are observed frequently in a variety of tumors, with UCES having the highest occurrence. Altogether, our study may provide a strategy and biomarker for clinical diagnosis, prognostics, and treatment of cancers by targeting GSDME.

Supplementary Information

The online version contains supplementary material available at https://doi.org/10.1186/s12935-024-03467-2.

Supplementary Material 1

Acknowledgements
The authors thank the people from the Research Center for Preclinical Medicine in Southwest Medical University.

Author contributions
J.F. developed the study concept and design; J.C., L.Z., D.L., and Ji. F. conducted sample collection and the experimental studies. J.C., M.M., and J. F. conducted bioinformatics analysis. J.C., Ji.F., M.M., and J. F. conducted manuscript preparation and editing; All authors reviewed the manuscript and approved its submission.

Funding
This study was partially funded by the National Natural Science Foundation of China (Nos. 82073263, 81672887, 31701087, and 30371493), the Foundation of Science and Technology Department of Sichuan Province (grant no. 2023NSFSC0673), the Joint Innovation Special Project of Science and Technology Plan of Sichuan Province (grant no. 2022YFS0623), the Joint Research Foundation of Luzhou City and Southwest Medical University (grant no. 23YKDYYJC0021), and the Project Fund for Young Innovative Talents of Huai'an No. 1 Hospital Affiliated to Nanjing Medical University (grant no. QC202209).

Data availability
Not applicable.

Declarations

Ethical approval
The study was approved by the Ethical Committee of Southwest Medical University and the Affiliated Huaian No. 1 People's Hospital of Nanjing Medical University for human studies and written informed consent was obtained from participants. All written informed consents and procedures adhered to the tenets of the Declaration of Helsinki.

Consent to participate
Obtained.

Consent for publication
Not applicable.

Informed consent
Informed consent was obtained from subjects involved in the study.

Institutional Review Board Statement
This study was performed in line with the principles of the Declaration of Helsinki and approval by the Southwest Medical University ethics committee.

Conflict of interest
The authors have no conflicts of interest to declare.

Author details
[1]Key Laboratory of Epigenetics and Oncology, The Research Center for Preclinical Medicine, Southwest Medical University, Luzhou 646000, Sichuan Province, P R China
[2]School of Basic Medical Sciences, Southwest Medical University, Luzhou 646000, Sichuan Province, China
[3]Department of Pathology, The Affiliated Huai'an No. 1 People's Hospital of Nanjing Medical University, Huai'an 223300, Jiangsu Province, China

Received: 28 July 2023 / Accepted: 29 July 2024
Published online: 08 August 2024

References

1. Thompson DA, Weigel RJ. Characterization of a gene that is inversely correlated with estrogen receptor expression (ICERE-1) in breast carcinomas. Eur J Biochem. 1998;252(1):169–77.
2. van Camp G, Coucke P, Balemans W, van Velzen D, van de Bilt C, van Laer L, Smith RJ, Fukushima K, Padberg GW, Frants RR, et al. Localization of a gene for non-syndromic hearing loss (DFNA5) to chromosome 7p15. Hum Mol Genet. 1995;4(11):2159–63.
3. Van Laer L, Huizing EH, Verstreken M, van Zuijlen D, Wauters JG, Bossuyt PJ, Van de Heyning P, McGuirt WT, Smith RJ, Willems PJ, et al. Nonsyndromic hearing impairment is associated with a mutation in DFNA5. Nat Genet. 1998;20(2):194–7.
4. Huizing EH, van Bolhuis AH, Odenthal DW. Studies on progressive hereditary perceptive deafness in a family of 335 members. I. Genetical and general audiological results. Acta Otolaryngol. 1966;61(1):35–41.
5. Huizing EH, van Bolhuis AH, Odenthal DW. Studies on progressive hereditary perceptive deafness in a family of 335 members. II. Characteristic pattern of hearing deterioration. Acta Otolaryngol. 1966;61(1):161–7.
6. Mehl AL, Thomson V. Newborn hearing screening: the great omission. Pediatrics. 1998;101(1):E4.
7. Liu Y, Tan M, Cai L, Lv L, Chen Q, Chen W, Yang H, Xu Y. Genetic profiles of non-syndromic severe-profound hearing loss in Chinese Hans by whole-exome sequencing. Gene. 2022;819:146258.
8. Aboagye ET, Adadey SM, Wonkam-Tingang E, Amenga-Etego L, Awandare GA, Wonkam A. Global Distribution of Founder Variants Associated with non-syndromic hearing impairment. Genes (Basel). 2023;14(2):14.
9. Cheng J, Li T, Tan Q, Fu J, Zhang L, Yang L, Zhou B, Yang L, Fu S, Linehan AG, et al. Novel, pathogenic insertion variant of GSDME associates with autosomal dominant hearing loss in a large Chinese pedigree. J Cell Mol Med. 2024;28(1):e18004.
10. Op de Beeck K, Van Camp G, Thys S, Cools N, Callebaut I, Vrijens K, Van Nassauw L, Van Tendeloo VF, Timmermans JP, Van Laer L. The DFNA5 gene, responsible for hearing loss and involved in cancer, encodes a novel apoptosis-inducing protein. Eur J Hum Genet. 2011;19(9):965–73.
11. De Schutter E, Croes L, Ibrahim J, Pauwels P, Op de Beeck K, Vandenabeele P, Van Camp G. GSDME and its role in cancer: from behind the scenes to the front of the stage. Int J Cancer. 2021;148(12):2872–83.
12. Kim MS, Chang X, Yamashita K, Nagpal JK, Baek JH, Wu G, Trink B, Ratovitski EA, Mori M, Sidransky D. Aberrant promoter methylation and tumor suppressive activity of the DFNA5 gene in colorectal carcinoma. Oncogene. 2008;27(25):3624–34.
13. Zhang Z, Zhao S, Yang H, Chen Y, Feng H, An M, Chen B. Prognostic and immunological role of gasdermin E in Pan-cancer Analysis. Front Oncol. 2021;11:706266.
14. Zhang Z, Zhang Y, Xia S, Kong Q, Li S, Liu X, Junqueira C, Meza-Sosa KF, Mok TMY, Ansara J, et al. Gasdermin E suppresses tumour growth by activating anti-tumour immunity. Nature. 2020;579(7799):415–20.
15. Rogers C, Fernandes-Alnemri T, Mayes L, Alnemri D, Cingolani G, Alnemri ES. Cleavage of DFNA5 by caspase-3 during apoptosis mediates progression to secondary necrotic/pyroptotic cell death. Nat Commun. 2017;8:14128.

16. Shi J, Zhao Y, Wang K, Shi X, Wang Y, Huang H, Zhuang Y, Cai T, Wang F, Shao F. Cleavage of GSDMD by inflammatory caspases determines pyroptotic cell death. Nature. 2015;526(7575):660–5.
17. Kong Q, Zhang Z. Cancer-associated pyroptosis: a new license to kill tumor. Front Immunol. 2023;14:1082165.
18. Wang J, Sun Z, Xie J, Ji W, Cui Y, Ai Z, Liang G. Inflammasome and pyroptosis in autoimmune liver diseases. Front Immunol. 2023;14:1150879.
19. Privitera G, Rana N, Armuzzi A, Pizarro TT. The gasdermin protein family: emerging roles in gastrointestinal health and disease. Nat Rev Gastroenterol Hepatol. 2023;20(6):366–87.
20. Fu J, Song B, Du J, Liu S, He J, Xiao T, Zhou B, Li D, Liu X, He T, et al. Impact of BSG/CD147 gene expression on diagnostic, prognostic and therapeutic strategies towards malignant cancers and possible susceptibility to SARS-CoV-2. Mol Biol Rep. 2023;50(3):2269–81.
21. Liu S, Yang L, Fu J, Li T, Zhou B, Wang K, Wei C, Fu J. Comprehensive analysis, immune, and cordycepin regulation for SOX9 expression in pan-cancers and the matched healthy tissues. Front Immunol. 2023;14:1149986.
22. Zhang H, Dong X, Ding X, Liu G, Yang F, Song Q, Sun H, Chen G, Li S, Li Y, et al. Bufalin targeting CAMKK2 inhibits the occurrence and development of intrahepatic cholangiocarcinoma through Wnt/beta-catenin signal pathway. J Transl Med. 2023;21(1):900.
23. Chen G, Zhang H, Sun H, Ding X, Liu G, Yang F, Feng G, Dong X, Zhu Y, Wang X, et al. Bufalin targeting BFAR inhibits the occurrence and metastasis of gastric cancer through PI3K/AKT/mTOR signal pathway. Apoptosis. 2023;28(9–10):1390–405.
24. Cunningham KG, Manson W, Spring FS, Hutchinson SA. Cordycepin, a metabolic product isolated from cultures of cordyceps militaris (Linn.) Link. Nature. 1950;166(4231):949.
25. Radhi M, Ashraf S, Lawrence S, Tranholm AA, Wellham PAD, Hafeez A, Khamis AS, Thomas R, McWilliams D, de Moor CH. A systematic review of the Biological effects of Cordycepin. Molecules. 2021;26(19):5886.
26. Liu Y, Guo ZJ, Zhou XW. Chinese cordyceps: Bioactive Components, Antitumor effects and underlying Mechanism-A review. Molecules. 2022;27(19):6576.
27. Tan L, Song X, Ren Y, Wang M, Guo C, Guo D, Gu Y, Li Y, Cao Z, Deng Y. Anti-inflammatory effects of cordycepin: a review. Phytother Res 2020.
28. Das G, Shin HS, Leyva-Gomez G, Prado-Audelo MLD, Cortes H, Singh YD, Panda MK, Mishra AP, Nigam M, Saklani S, et al. Cordyceps spp.: a review on its Immune-Stimulatory and other Biological potentials. Front Pharmacol. 2020;11:602364.
29. Wei C, Yao X, Jiang Z, Wang Y, Zhang D, Chen X, Fan X, Xie C, Cheng J, Fu J, et al. Cordycepin inhibits drug-resistance non-small cell Lung Cancer Progression by activating AMPK Signaling Pathway. Pharmacol Res. 2019;144:79–89.
30. Wei C, Khan MA, Du J, Cheng J, Tania M, Leung EL, Fu J. Cordycepin inhibits triple-negative breast Cancer Cell Migration and Invasion by regulating EMT-TFs SLUG, TWIST1, SNAIL1, and ZEB1. Front Oncol. 2022;12:898583.
31. Uhlen M, Fagerberg L, Hallstrom BM, Lindskog C, Oksvold P, Mardinoglu A, Sivertsson A, Kampf C, Sjostedt E, Asplund A et al. Proteomics. Tissue-based map of the human proteome. *Science* 2015, 347(6220):1260419.
32. Uhlen M, Zhang C, Lee S, Sjostedt E, Fagerberg L, Bidkhori G, Benfeitas R, Arif M, Liu Z, Edfors F et al. A pathology atlas of the human cancer transcriptome. *Science* 2017, 357(6352).
33. Tang Z, Li C, Kang B, Gao G, Li C, Zhang Z. GEPIA: a web server for cancer and normal gene expression profiling and interactive analyses. Nucleic Acids Res. 2017;45(W1):W98–102.
34. Tang Z, Kang B, Li C, Chen T, Zhang Z. GEPIA2: an enhanced web server for large-scale expression profiling and interactive analysis. Nucleic Acids Res. 2019;47(W1):W556–60.
35. Fu J, Wei C, He J, Zhang L, Zhou J, Balaji KS, Shen S, Peng J, Sharma A, Fu J. Evaluation and characterization of HSPA5 (GRP78) expression profiles in normal individuals and cancer patients with COVID-19. Int J Biol Sci. 2021;17(3):897–910.
36. Cerami E, Gao J, Dogrusoz U, Gross BE, Sumer SO, Aksoy BA, Jacobsen A, Byrne CJ, Heuer ML, Larsson E, et al. The cBio cancer genomics portal: an open platform for exploring multidimensional cancer genomics data. Cancer Discov. 2012;2(5):401–4.
37. Ding W, Feng G, Hu Y, Chen G, Shi T. Co-occurrence and mutual exclusivity analysis of DNA methylation reveals distinct subtypes in multiple cancers. Front Cell Dev Biol. 2020;8:20.
38. Abutalebi M, Li D, Ahmad W, Mokhtari K, Entezari M, Hashemi M, Fu J, Maghsoudloo M. Discovery of PELATON links to the INHBA gene in the TGF-beta pathway in colorectal cancer using a combination of bioinformatics and experimental investigations. Int J Biol Macromol. 2024;270(Pt 1):132239.
39. Fu J, Liu S, Tan Q, Liu Z, Qian J, Li T, Du J, Song B, Li D, Zhang L, et al. Impact of TMPRSS2 expression, mutation prognostics, and small molecule (CD, AD, TQ, and TQFL12) inhibition on Pan-cancer tumors and susceptibility to SARS-CoV-2. Molecules. 2022;27(21):7413.
40. Li D, Liu X, Zhang L, He J, Chen X, Liu S, Fu J, Fu S, Chen H, Fu J, et al. COVID-19 disease and malignant cancers: the impact for the furin gene expression in susceptibility to SARS-CoV-2. Int J Biol Sci. 2021;17(14):3954–67.
41. Zhou J, Imani S, Shasaltaneh MD, Liu S, Lu T, Fu J. PIK3CA hotspot mutations p. H1047R and p. H1047L sensitize breast cancer cells to thymoquinone treatment by regulating the PI3K/Akt1 pathway. Mol Biol Rep. 2022;49(3):1799–816.
42. Yokomizo K, Harada Y, Kijima K, Shinmura K, Sakata M, Sakuraba K, Kitamura Y, Shirahata A, Goto T, Mizukami H, et al. Methylation of the DFNA5 gene is frequently detected in colorectal cancer. Anticancer Res. 2012;32(4):1319–22.
43. Kim MS, Lebron C, Nagpal JK, Chae YK, Chang X, Huang Y, Chuang T, Yamashita K, Trink B, Ratovitski EA, et al. Methylation of the DFNA5 increases risk of lymph node metastasis in human breast cancer. Biochem Biophys Res Commun. 2008;370(1):38–43.
44. Ding W, Chen G, Shi T. Integrative analysis identifies potential DNA methylation biomarkers for pan-cancer diagnosis and prognosis. Epigenetics. 2019;14(1):67–80.
45. Huang PY, Shih IA, Liao YC, You HL, Lee MJ. A novel HDAC11 inhibitor potentiates the tumoricidal effects of cordycepin against malignant peripheral nerve sheath tumor through the Hippo signaling pathway. Am J Cancer Res. 2022;12(2):873–92.
46. Rogers C, Erkes DA, Nardone A, Aplin AE, Fernandes-Alnemri T, Alnemri ES. Gasdermin pores permeabilize mitochondria to augment caspase-3 activation during apoptosis and inflammasome activation. Nat Commun. 2019;10(1):1689.
47. Khan MA, Tania M. Cordycepin in Anticancer Research: molecular mechanism of Therapeutic effects. Curr Med Chem. 2020;27(6):983–96.
48. Ozdemir ES, Gomes MM, Fischer JM. Computational modeling of TP63-TP53 Interaction and Rational design of inhibitors: implications for therapeutics. Mol Cancer Ther. 2022;21(12):1846–56.
49. Ying L, Hao M, Zhang Z, Guo R, Liang Y, Yu C, Yang Z. Medicarpin suppresses proliferation and triggeres apoptosis by upregulation of BID, BAX, CASP3, CASP8, and CYCS in glioblastoma. Chem Biol Drug Des. 2023;102(5):1097–109.
50. Eskandari E, Eaves CJ. Paradoxical roles of caspase-3 in regulating cell survival, proliferation, and tumorigenesis. J Cell Biol. 2022;221(6):e202201159.
51. Wang S-F, Tseng L-M, Lee H-C. Role of mitochondrial alterations in human cancer progression and cancer immunity. J Biomed Sci. 2023;30(1):61.
52. Wei X, Xie F, Zhou X, Wu Y, Yan H, Liu T, Huang J, Wang F, Zhou F, Zhang L. Role of pyroptosis in inflammation and cancer. Cell Mol Immunol. 2022;19(9):971–92.
53. Jang I, Beningo KA. Integrins, CAFs and mechanical forces in the progression of cancer. Cancers. 2019;11(5):721.
54. Hayward M-K, Muncie JM, Weaver VM. Tissue mechanics in stem cell fate, development, and cancer. Dev Cell. 2021;56(13):1833–47.
55. Jiang M, Qi L, Li L, Li Y. The caspase-3/GSDME signal pathway as a switch between apoptosis and pyroptosis in cancer. Cell Death Discov. 2020;6:112.
56. Liu Z, Liu H, Dong Q, Li H, Zhang B, Liu Y, Zhong L, Tang H. Prognostic role of DFNA5 in head and neck squamous cell carcinoma revealed by systematic expression analysis. BMC Cancer. 2021;21(1):951.
57. Li S, Yue M, Xu H, Zhang X, Mao T, Quan M, Ma J, Wang Y, Ge W, Wang Y, et al. Chemotherapeutic drugs-induced pyroptosis mediated by gasdermin E promotes the progression and chemoresistance of pancreatic cancer. Cancer Lett. 2023;564:216206.
58. Li D, Cheng J, Zhang W, Zhang L, Maghsoudloo M, Fu J, Liu X, Xiao X, Wei C, Fu J. Tripartite motif-containing 28 (TRIM28) expression and cordycepin inhibition in progression, prognosis, and therapeutics of patients with breast invasive carcinoma. J Cancer. 2024;15(13):4374–85.
59. Nakamura K, Shinozuka K, Yoshikawa N. Anticancer and antimetastatic effects of cordycepin, an active component of Cordyceps Sinensis. J Pharmacol Sci. 2015;127(1):53–6.
60. Yoshikawa N, Kunitomo M, Kagota S, Shinozuka K, Nakamura K. Inhibitory effect of cordycepin on hematogenic metastasis of B16-F1 mouse melanoma cells accelerated by adenosine-5′-diphosphate. Anticancer Res. 2009;29(10):3857–60.

61. Nakamura K, Yoshikawa N, Yamaguchi Y, Kagota S, Shinozuka K, Kunitomo M. Antitumor effect of cordycepin (3'-deoxyadenosine) on mouse melanoma and lung carcinoma cells involves adenosine A3 receptor stimulation. Anticancer Res. 2006;26(1A):43–7.
62. Tuli HS, Sharma AK, Sandhu SS, Kashyap D. Cordycepin: a bioactive metabolite with therapeutic potential. Life Sci. 2013;93(23):863–9.
63. Tuli HS, Sandhu SS, Sharma AK. Pharmacological and therapeutic potential of cordyceps with special reference to Cordycepin. 3 Biotech. 2014;4(1):1–12.
64. Du J, Fu J, Zhang W, Zhang L, Chen H, Cheng J, He T, Fu J. Effect of DPP4/CD26 expression on SARS–CoV–2 susceptibility, immune response, adenosine (derivatives m(6)(2)A and CD) regulations on patients with cancer and healthy individuals. Int J Oncol. 2023;62(3):41.
65. Li T, Luo N, Fu J, Du J, Liu Z, Tan Q, Zheng M, He J, Cheng J, Li D, et al. Natural product cordycepin (CD) inhibition for NRP1/CD304 expression and possibly SARS-CoV-2 susceptibility Prevention on cancers. Microorganisms. 2023;11(12):2953.
66. Taghinejad Z, Kazemi T, Fadaee M, Farshdousti Hagh M, Solali S. Pharmacological and therapeutic potentials of cordycepin in hematological malignancies. Biochem Biophys Res Commun. 2023;678:135–43.
67. Liu G, Yang L, Chen G, Xu F, Yang F, Yu H, Li L, Dong X, Han J, Cao C, et al. A review on Drug Delivery System for Tumor Therapy. Front Pharmacol. 2021;12:735446.

Publisher's Note